Astron. Astrophys. 338, 151–160 (1998)

ASTRONOMY AND ASTROPHYSICS

On-line determination of stellar atmospheric parameters $T_{\rm eff}$, $\log g$, [Fe/H] from ELODIE echelle spectra*

I. The method

D. Katz[1], **C. Soubiran**[2], **R. Cayrel**[1], **M. Adda**[3], **and R. Cautain**[4]

[1] Observatoire de Paris, DASGAL, 61 av. de l'Observatoire, F-75014 Paris, France
[2] Observatoire de Bordeaux, BP89, F-33270 Floirac, France
[3] Observatoire de Paris-Meudon, DESPA, F-92195 Meudon Cedex, France
[4] Observatoire de Haute-Provence, F-04870 Saint-Michel l'Observatoire, France

Received 20 April 1998 / Accepted 12 June 1998

Abstract. We present a method estimating the atmospheric parameters $T_{\rm eff}$, $\log g$, [Fe/H] for stars observed, even at low signal to noise ratio, with the echelle spectrograph ELODIE on the 193cm telescope at Observatoire de Haute-Provence. The method relies on the least-square comparison of the spectrum of a target star to a library of 211 spectra of reference stars for which the atmospheric parameters are well known and which were observed with the same instrument. In order to obtain a meaningful comparison between target and reference spectra, all features which are not intrinsic to the objects must be removed. This treatment involves the correction of the blaze efficiency for each order, cosmic rays hits and telluric line removal, convolution of the spectra to a common spectral resolution, wavelength scale and flux level adjustment. The library available at the present time covers the effective temperature range [4000K, 6300K], the metallicity range [−2.9, +0.35] and the gravities of both unevolved and evolved stars existing at these temperatures and metallicities. Tests performed with the actual library allow us to estimate the internal accuracy to be 86 K, 0.28 dex and 0.16 dex for $T_{\rm eff}$, $\log g$, [Fe/H] for a target star with S/N = 100 and 102 K, 0.29 dex and 0.17 dex at S/N = 10. This accuracy will improve in the future as the number of reference stars in the library will increase. The software (named TGMET) has been installed at Observatoire de Haute-Provence for the on-line analysis of the high-resolution spectra of ELODIE, which was originally conceived for accurate radial velocity measurements.

Key words: methods: data analysis – methods: numerical – stars: abundances – stars: atmospheres – stars: fundamental parameters

1. Introduction

The availability of immediate, on-line reduction for radial velocities at the ELODIE echelle-spectrograph of the Observatoire de Haute-Provence, led to the obvious idea that it would be very useful to extend this type of fast analysis to other stellar parameters. Being ourselves involved in the determination of the metallicity of stars of known proper motions in two galactic directions (Soubiran 1992, Ojha et al. 1994, Perrin et al. 1995) we were tempted to try to determine on-line the metallicity, effective temperature and gravity of a star observed with ELODIE. Our former experience with this type of determination from spectra at a lower resolution from a grid of synthetic spectra (Cayrel et al. 1991a & b, Perrin et al. 1995) allowed us to estimate that for old stars (with slow rotation) of solar type or cooler, a mean accuracy of 200 K in $T_{\rm eff}$, 0.4 dex in gravity and 0.3 dex in metallicity was possible from a spectrum obtained with a signal to noise ratio (S/N) of 50 on a limited spectral interval. From theoretical considerations (Cayrel 1991) we thought that with the higher resolution and larger spectral interval of ELODIE's spectra, it would be possible to obtain comparable or better precision on low S/N ($\sim$ 10) spectra.

We could have followed the same approach as before, and tried to compare the observed spectrum with a grid of synthetic spectra, generated for example with the ATLAS9, SYNTHE (Kurucz 1993) codes made generously available to us by R.L. Kurucz. However we thought that there was a simpler method, i.e. comparing the spectrum of the target star with a library of spectra of reference stars, with accurately determined parameters, taken with the same spectrograph. The disadvantage is that an error on the parameters of reference stars affects the result. Also the optimal extraction of the parameters possible with a grid of synthetic spectra, where the sensitivity of any spectral feature to the parameters is known explicitly, is lost. The advantage is that a very large spectral range can be used, without the very tedious work of fine-tuning the oscillator strengths and damping constants of an extremely large number of atomic or molecular lines. This approach would also avoid the empirical corrections of synthetic to reference star spectra that have proven to be necessary (Cuisinier et al. 1994).

The principle sounds very simple. But, before the target spectrum can be meaningfully compared to the spectra of the

Send offprint requests to: D. Katz, (david.katz@obspm.fr)

* based on observations made on the 193cm telescope at Observatoire de Haute-Provence, France

library, many steps are required. First of all it is necessary to remove all features which are not specific to the object, but instrumental in nature, or associated to particular conditions of observation (Sect. 3). The main instrumental feature is the modulation of the spectra by the blaze profile of each order. If the two objects to be compared had the same radial velocity with respect to the instrument, at the time of the exposures, this modulation would cancel out. But most of the time there is a significant difference, and the blaze efficiency is shifted in wavelength between the two exposures. This modulation must be corrected (Sect. 3.2). Cosmic rays are a big nuisance in all instruments using CCDs as detectors. A first treatment is made in the radial-velocity software (Baranne et al. 1996), following Horne's algorithm (1986). Unfortunately many cosmics escape the trap, because too few pixels are illuminated along the direction perpendicular to the dispersion. Therefore the remaining cosmics must be chased (Sect. 3.3). Equally disturbing are the telluric lines which change in intensity and position with time in the rest frame of the object. The pixels affected by these wandering disturbers must be eliminated (Sect. 3.6). If the night is spoiled by the Moon, it may be necessary to subtract a sky exposure, for which all the steps already described (except telluric line removal) must be carried out too (Sect. 3.4).

After these different steps, three other actions remain to be performed. Two spectra to be compared must be brought:

(i) to the same spectral resolution
(ii) to a common wavelength scale
(iii) to a common level of flux

If the target star and a reference star of the library have a different line-broadening, because they have a different projected rotational velocity $v \sin i$, we must not be fooled into considering them as objects of different effective temperature, gravity and metallicity. Also it is not guaranteed that the instrumental resolution is exactly the same for all observing runs (e.g. because of focus variations). Therefore all the spectra of the library and the target's star are forced to a common resolution (action (i) listed above), in order to eliminate spectral differences originating from projected rotation, macroturbulence or instrumental resolution (Sect. 3.5).

Action (ii) is easy to perform because the radial velocity of the target star and of each comparison star is accuratly known from the radial velocity software (Baranne et al. 1996), by cross-correlation with a mask (Sect. 4.1). Action (iii) is done by least squares (Sect. 4.2).

A large fraction of our observing time was devoted to the acquisition of the library of reference stars, which includes 211 spectra at the present time. Sect. 2 describes the observational material. A detailed description of the library is available in a companion paper (Soubiran et al. 1998, hereafter Paper II). The spectra of this library are available at the CDS Strasbourg, together with their revised atmospheric parameters (Sect. 5).

Different tests have been performed to evaluate the consistency and the accuracy of the method (Sect. 6).

The software is named TGMET, for Temperature, Gravity, METallicity.

2. ELODIE's spectra

ELODIE is a fibre-fed spectrograph devoted to the measurements of accurate radial velocities (Baranne et al. 1996). It has been in operation since 1993 on the 193cm telescope of Observatoire de Haute-Provence. The most striking result of this instrument is the discovery of the first jovian planet orbiting the solar-type star 51 Peg (Mayor & Queloz 1995). Its resolution power is 42000, the spectra range from 390 nm to 680 nm and are recorded as 67 orders (numbered from 91 to 157) on a 1024×1024 Techtronic's CCD. The reduction of the spectra is automatically performed on-line, as well as the computation of radial velocities by cross-correlation thanks to the ELODIE reduction software developed by D. Queloz (1996). The precision of radial velocities is about 100 m.s^{-1} for F, G and K stars. A typical S/N of 100 is achieved with one hour exposure on a 8.5^{th} magnitude star or a S/N of 10 on a 12.75^{th} magnitude star, taking into account a read noise of 8 e$^-$ per CCD pixel or 15 e$^-$ per spectral resolution element. The different configurations of ELODIE are very stable, allowing to compare easily spectra observed at different epochs.

To develop this method, we have observed, between 1994 and 1997, 250 reference stars at a mean S/N of 100, 211 of which remained in the final library. We have also observed at low S/N (4 to 30) 30 well-known stars with various atmospheric parameters to test the software. In parallel, we have achieved our primary objective which was to probe the Galactic stellar populations in two directions, where we observed 132 stars of our astrometric program (Soubiran 1993, Ojha et al. 1994). Stars exhibiting a double correlation peak (identifying themselves as spectroscopic binaries) during the radial velocity determination, were removed from the set of observations. We have worked on already extracted spectra, i.e. on one-dimensional spectra, of 1024 spectral elements per order. We will call pixel any of these spectral elements along a given order, although it is not a CCD pixel anymore.

3. Preparation of the spectra

3.1. Wavelength calibration

The extraction of the orders and the calculation of the coefficients of interpolation for the wavelength calibration are performed, just after the exposure, by the ELODIE reduction software. These coefficients are used in formula (1) to establish the relation between pixels and wavelengths.

$$\lambda(x,k) = \frac{1}{k} \sum_{i=0}^{3} \sum_{j=0}^{5} A(i,j) T_i(\tilde{x}) T_j(\tilde{k}^{-1}) \qquad (1)$$

where $k \in [91, 157]$ is the order of the spectrum, $x \in [1, 1024]$ the number of the pixel in a given order, T_i and T_j the values of the Chebyshev polynomial of order i and j at the

points $\tilde{x}$ and $\tilde{k}^{-1}$ and $A(i,j)$ the coefficients of the interpolation. In Eq. (1), $\tilde{x}$ and $\tilde{k}^{-1}$ are x and 1/k normalized on the $[-1,1]$ interval by a linear transformation.

3.2. Flat field correction and straightening of each order

The ELODIE reduction software provides a flat field correction, separated in two components. The first one is the response correction, that takes into account pixel to pixel sensitivity differencies. The extracted spectra we are using underwent this correction. The second one is a division of each order by the response of the tungsten lamp spectrum of the same order, to correct the spectra from the modulation of the blaze profile.

We decided not to use the same procedure to straighten the orders, because of the presence of a coloured filter in the beam. This filter is necessary to balance the exposures at the red end and the violet end of the tungsten lamp. But it implies that the spectrum is not flat along the wavelength coordinate. Therefore, polynomials of order 7 to 19 were fitted to the continuum of four very metal-poor (almost line-free) stars: HD 221170, [Fe/H] = -2.10, HD 216143, [Fe/H] = -2.15, HD 108317, [Fe/H] = -2.36, HD 140283, [Fe/H] = -2.53 (Soubiran et al. 1998, Paper II). For each order k, the response curve $B_k(x)$ is given by the polynomial which is less affected by the spectral lines, with respect to the three others. Instead of using the tungsten response, the observed spectra are straightened by dividing their flux, order by order, pixel by pixel, by $B_k(x)$, normalized at 1 at its maximum. For further uses all the pixels that correspond to a response value lower than 0.5 at the edges of the orders are rejected by giving them the flag value -100.0.

Orders 138 to 157 (the bluest spectral orders) were rejected, because they were underilluminated with respect to the rest of the orders, and too much degraded by noise.

If the spectral energy distribution (SED) of the target star is very similar to that of the star which was used for straightening the order, no significant slope in the SED of the straightened order is expected. If the two stars have different colours, a residual slope is expected. Initially, the adjustement of the slope between the target and a reference star was performed in the least square fit of the flux levels. However a better consistency was attained in removing this adjustment. In practice the slope remains very small over an order: about 1% from edge to edge for a 1200 K difference in effective temperature. The "successful" comparison star has of course a temperature difference considerably smaller than this, with respect to the target star, so the slope adjustment is not necessary. Indeed it is even unwise, because if slope adjustment is provided, the software try to compensate the presence of a strong line at the edge of an order in a comparison star, by inventing an unphysical strong slope in the target star, when the line is non-existent or much weaker in the target star (or vice versa). Fig. 1 shows order 100 of HD 25329 before and after straightening.

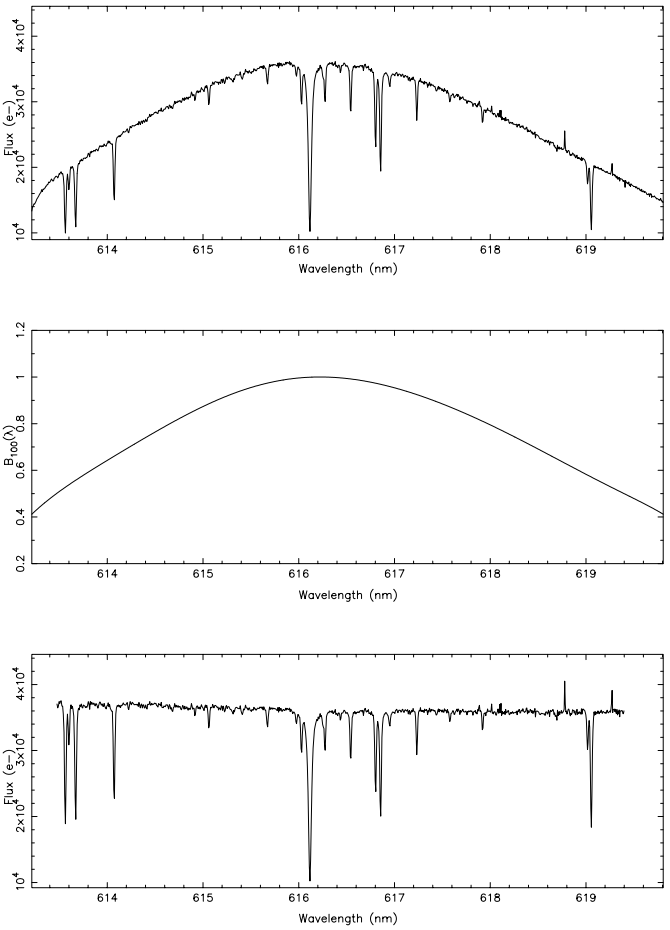

Fig. 1. Order 100 of HD 25329 ($T_{\rm eff}$ = 4787 K, $\log g$ = 4.58, [Fe/H] = -1.72, S/N = 141) before (top) and after straightening (bottom) and the response curve $B_{100}(\lambda)$ which has been used to straighten the order (middle).

3.3. Cosmic rays and defective pixels removal

The ELODIE reduction software corrects the 2D frames from the cosmic rays (high energy particles hitting the CCD), and from the defective pixels (pixels with reduced sensitivity), with the optimal extraction method of Horne (1986). As the flux profile, perpendicular to the direction of dispersion, is known, the Horne's method corrects the pixels which do not match this profile.

But in the case of ELODIE, the width of the orders, perpendicular to the direction of dispersion, is very thin (3 to 5 pixels). In this case Horne's method misses a significant part of the cosmics and defective pixels (up to 200 cosmics detectable for a one hour exposure and $S/N \simeq 50$). To remove the remaining "bad" pixels, we are using three different and complementary methods on the 1D spectra. Fig. 2 shows an order before and after cosmic rays and defective pixels removal.

3.3.1. The flux method

For the stars we are observing ($4000K \leq T_{\rm eff} \leq 6300K$) and in the wavelength interval we are using (440 nm to 680 nm)

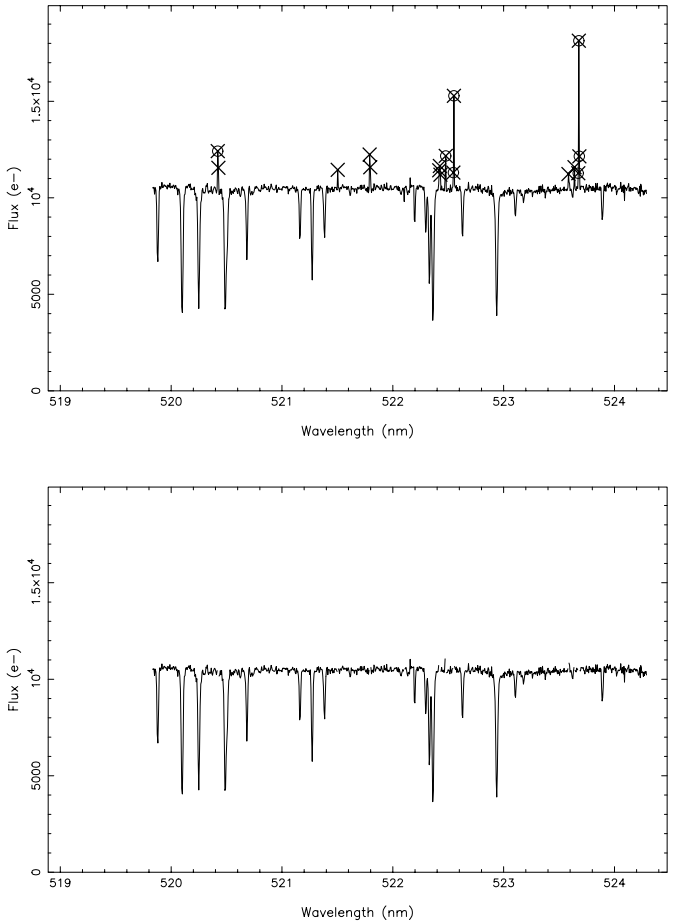

Fig. 2. Order 118 of HD 64090 ($T_{\rm eff}$ = 5446 K, $\log g$ = 4.45, [Fe/H] = -1.76, S/N = 106) before and after cosmic rays and defective pixels removal. Crosses flag cosmics detected by the flux method, circles flag cosmics detected by the regularity check method.

the lines are only in absorption. So, every feature that overruns the continuum by more than the Poisson photon noise has to be removed. This assumes that the continuum is well defined.

In metal-rich stars the lines are so numerous that the mean and median values of the flux seriously underestimate the continuum. There are so few true continuum points that they cannot be successfully fit by a least-squares approach. Instead, the continuum is estimated by the value of the 50^{th} highest pixel of the order. A highest pixel was not chosen to avoid the strongest part of the Poisson photon noise. But in the most metal rich stars, even the value of the 50^{th} pixel slightly underestimates the continuum. Therefore an index has been defined, which is the number of pixels included between the continuum plus one sigma and the continuum minus five sigma, divided by the total number of pixels of the order. We have assumed Poisson noise statistics, and taken sigma equal to the square root of the estimated continuum expressed in number of photo-electrons. This index is well correlated with the difference between the true and the estimated continuum, because it gives an insight of the number and width of the lines which affect the shape of an order. An order with a few small lines will have a high value of its index and a continuum well estimated, whereas an order with many broad lines will have a small value of its index, few points belonging to the true continuum (often less than 50) which will be underestimated. From the estimated continuum and the index, the limit of the Poisson photon noise is determined and the pixels with a higher value are removed, giving them the flag value -100.0.

This method is especially useful for the cosmic rays that fall in the continuum (as opposed to those that fall into the lines).

3.3.2. The regularity check method

The second method is used to find cosmics, wherever they fall, and the defective pixels. For every 4 consecutive pixels, a second order polynomial is fitted on their fluxes, by the least square method. It gives 4 residuals for each pixel. The 4 residuals are then quadratically summed to obtain a global rms deviation for each pixel. If a pixel belongs to the continuum, it will have a very small rms deviation because of the easiness to fit the continuum with a second order polynomial. If the pixel belongs to a portion of the spectrum containing stellar lines it will have, most of the time, a larger but still modest rms deviation, because the shape of the lines is an analytic function, correctly fitted by a second order polynomial over 4 consecutive points. If a pixel is defective, or has been hit by a cosmic, its value is very different from those of its neighbours. This change is so sharp, that it can't be well fitted by a second order polynomial, and then the pixel will have a high residual.

Then the mean absolute value of the residuals and their standard deviation σ_r over the order are calculated. Two cases are distinguished. If the pixel flux is above the estimated continuum determined by the flux method (Sect. 3.3.1), the pixel is suspected to have been hit by a cosmic and is removed if its residual exceeds the mean by more than $4.6\sigma_r$.

If the pixel flux is below the continuum, the pixel is a defective pixel candidate and is removed if its residual exceeds the mean by more than $11\sigma_r$. This latest high value of the rejection coefficient, comes from the fact, that in a portion containing few narrow lines the rms deviation gets close to those of segments containing defective pixels.

The elimination procedure is iterated until no more pixels are removed. As in the first method, removed pixels are flagged at -100.0.

3.3.3. The list of defective pixels

Because of the need to take a high value of the rejection coefficient in the case of defective pixel candidates, sometimes some of them are missed. The third method uses a list of recurrent defective pixels. They were detected in the stars with broad lines where they are easily distinguished. This list is taken as a map of the defective pixels of the CCD. Therefore, all the pixels of this list are assigned the flag value -100.0.

This list is unfortunately somewhat time dependent and is updated at each observing period. We recall that what is called pixel in the extracted 1D spectrum is indeed a spectral element

involving several true CCD pixels and is dependent on the position of the spectrum on the CCD.

3.4. Sky subtraction

The spectrum of the sky is straightened, cleaned of cosmics and defective pixels and subtracted pixel by pixel from the star spectrum. As the sky subtraction adds noise, it is suggested to performed it only if the skylight reaches at least 1% of the starlight.

3.5. Spectrum convolution

The average resolution power of ELODIE (42000) corresponds to a FWHM of 7.14 km.s^{-1} for the line-width. The actual FWHM of spectral lines is the convolution of the intrinsic line-width by this instrumental line-width. It turns out that the resulting line-width varies from star to star, but is most of the time between 10 and 13 km.s^{-1} for old F,G, and K stars. For a young star the FWHM can be much higher. The resulting resolution is measured by the FWHM of the cross-correlation function of the radial velocity determination ($2.35\sigma_{V_r}$, where σ_{V_r} is the standard deviation of the cross-correlation function of the star given by the ELODIE reduction software). As the template mask used for the correlation has a large number of lines, the accuracy on the radial velocity is much smaller than σ_{V_r}. For the temperature range of our stars, σ_{V_r} is usually smaller than 5.5 km.s^{-1}. In this case, to compare spectra at the same resolution, all the spectra (target and reference stars) were convolved by a gaussian of standard deviation: $\sqrt{5.5^2 - \sigma_{Vr}^2}$ km.s^{-1}.

Unfortunately for some hot stars ($T_{\rm eff} > 6100$ K), the σ_{V_r} reaches values higher than 5.5 km.s^{-1}. In this case TGMET is performed with versions of the library degraded to lower resolutions.

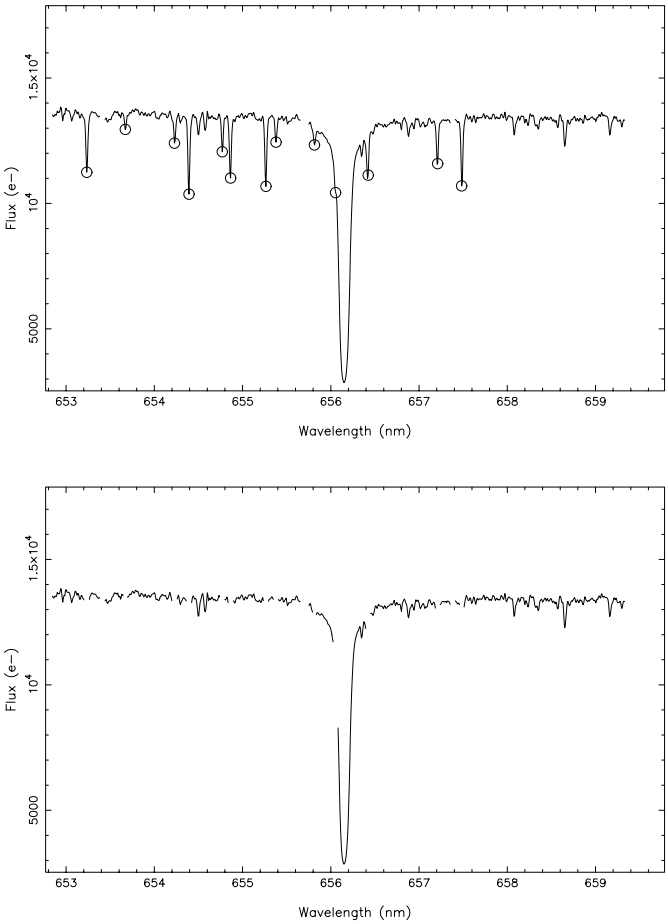

Fig. 3. Order 94 of HD 4306 ($T_{\rm eff}$ = 4975 K, $\log g$ = 2.01, [Fe/H] = -2.72, S/N = 89) before and after atmospheric lines removal. The circles are showing the wavelengths of the telluric lines as identified in the Rolland's table. The broad line at 656.28 nm is H_α.

3.6. Telluric lines removal

The stars are observed in different conditions of air mass and humidity and have different radial velocities with respect to the spectrograph. Therefore, positions with respect to the stellar lines and intensities of telluric lines are changing from one spectrum to another. They have to be removed to avoid any earth atmosphere contribution during the comparison between two spectra.

Telluric lines have been identified using the table of Rowland of "The solar spectrum" (Moore et al. 1966). Two or three pixels are removed on each side of the central pixel of each telluric line, depending on the equivalent width listed in the Rowland's solar spectrum: smaller or larger than 2 mÅ. Fig. 3 shows the order 94 of HD 4306 before and after telluric lines removal.

4. Method of comparison object / library

The principle of the method is very simple: once the spectrum of an unknown object is cleaned of instrumental effects, and spurious pixels or lines, it can be adjusted, order by order, pixel by pixel, against several reference spectra by a least square method. The reduced χ^2 of the fit is taken as a measure of resemblance between the target spectrum and a reference spectrum. There are two steps for this : *wavelength adjustment and signal amplitude adjustment.*

4.1. Wavelength adjustment

The target and a reference star have not the same radial velocity with respect to the spectrograph, and the first thing to do is to shift the spectrum of the reference star to the radial velocity of the object in order to make the absorption lines coincide exactly. As the difference in radial velocity does not correspond to a whole number of pixels, the flux corresponding to a given pixel of the shifted spectrum is not known and has to be interpolated. We chose to shift the reference spectrum instead of the contrary in order to avoid an interpolation on *a too noisy function*. A quadratic Bessel's interpolation formula was employed. It makes use of two points before and two points after the considered pixel x :

$$f(x) = (1-p)f(x_0) + pf(x_1) + A\frac{p(p-1)}{4}$$

where:

$$p = \frac{(x - x_0)}{(x_1 - x_0)}$$

$$x_{-1} < x_0 \leq x < x_1 < x_2$$

and:

$$A = f(x_2) + f(x_{-1}) - f(x_0) - f(x_1)$$

This formula is nicely insensitive to noise in the data: if the individual values are affected by a noise ϵ the expected noise on the interpolated value is at the most $(9/8)\epsilon$. High order formulae would be amplifying spectrum noise.

4.2. Mean flux adjustment

The fluxes of the target and reference stars being usually very different, one has to put them on a common scale. It was decided to move the reference spectrum to the mean level of the object spectrum. The first idea, based on theoretical considerations, was to solve this problem by weighted least-squares, finding u such that:

$$S_k = \frac{1}{n_k - 1} \sum_{i \in E_k} \left[\frac{F_{obj}(i,k) - u_k F_{ref}(i,k)}{\sigma_{i,k}} \right]^2$$

where:
$F_{obj}(i,k)$ is the flux of the target star at pixel i and order k. $F_{ref}(i,k)$ is the interpolated flux of a reference star interpolated at the same intrinsic wavelength, as explained in Sect. 4.1. E_k is the set of pixels of order k, for which none of the $F_{obj}(i,k)$ or $F_{ref}(i,k)$ are flagged at $-$ 100.0 value. n_k is the number of elements in E_k, typically 800 for a single order and $\sigma_{i,k}$ is the combined noise affecting the numerator flux difference.

Thence S_k is nothing else than the reduced χ^2 of the fit. In the particular case in which a perfect twin of the target star exists in the library (no intrinsic difference, impact of noise only) the expected value of χ^2 is 1, with a variance of $2/(n-1)$. It is of course advantageous to combine the χ^2 of several orders, because this is equivalent to increase n, and to decrease the noise $\sqrt{2/(n-1)}$. For example, with 10 orders, an intrinsic rms difference of only 1.5 per cent can, theoretically, be detected with an observational S/N of 10. The implementation needs some iterations, because the noise on the numerator depends upon u, not known at the beginning.

However, after many tests, described in the following section, it was found that good results could be obtained with a simpler equivalent technique. Instead of weighting the terms in the expression of S_k by $(\frac{1}{\sigma_{i,k}})^2$, we chose to weight them by the response curve B_k (see Sect. 3.2) which is proportional to $\frac{1}{\sigma^2}$ when the photon noise dominates, which is the case at $S/N > 10$. The least square adjustment may then be replaced by finding the value u_k for each order, which minimizes the expression :

$$S'_k = \frac{1}{n_k - 1} \sum_{i \in E_k} (F_{obj}(i,k) - u_k F_{ref}(i,k))^2 B_k(i)$$

giving lower weight to the edges of the order, in the right proportion. This leads to a simple formula to determine u:

$$u_k = \frac{\sum_{i \in E_k} F_{obj}(i,k) F_{ref}(i,k) B_k(i)}{\sum_{i \in E_k} F^2_{ref}(i,k) B_k(i)}$$

Then, the variance is calculated for each order. Fig. 4 shows the fit between HD 41597 and HD 40460 (stars with similar parameters) and Fig. 5 shows the fit between HD 41597 and HD 4628 (stars with different parameters).

Now comes the question of properly combining the information contained in the different orders. This is not a trivial

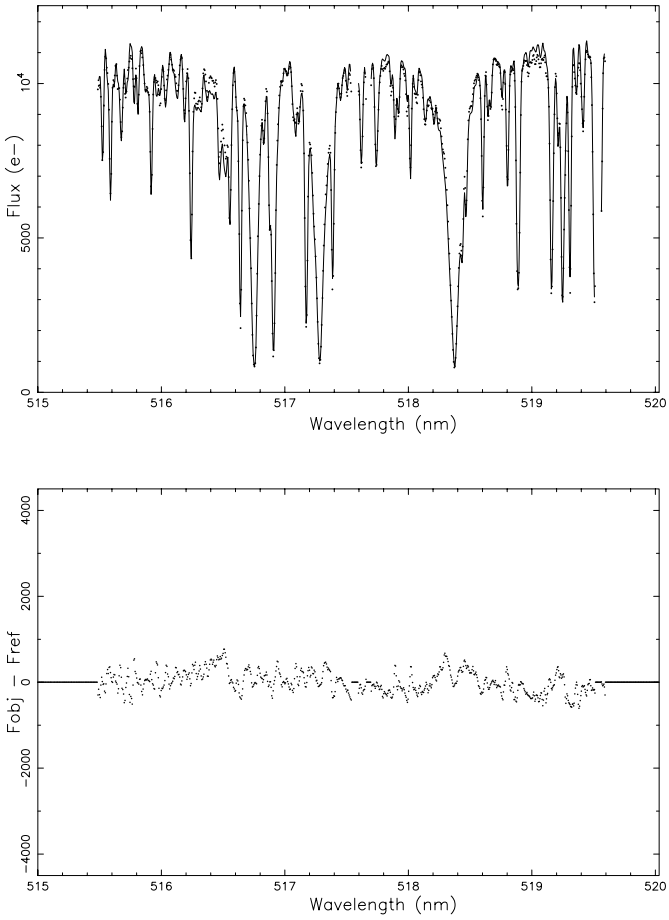

Fig. 4. The upper part of the figure shows the fit between HD 41597, in points, taken as the target ($T_{\rm eff}$ = 4700 K, $\log g$ = 2.38, [Fe/H] = -0.54) and HD 40460 taken as the reference star ($T_{\rm eff}$ = 4741 K, $\log g$ = 2.00, [Fe/H] = -0.50). The lower part shows the difference between their fluxes.

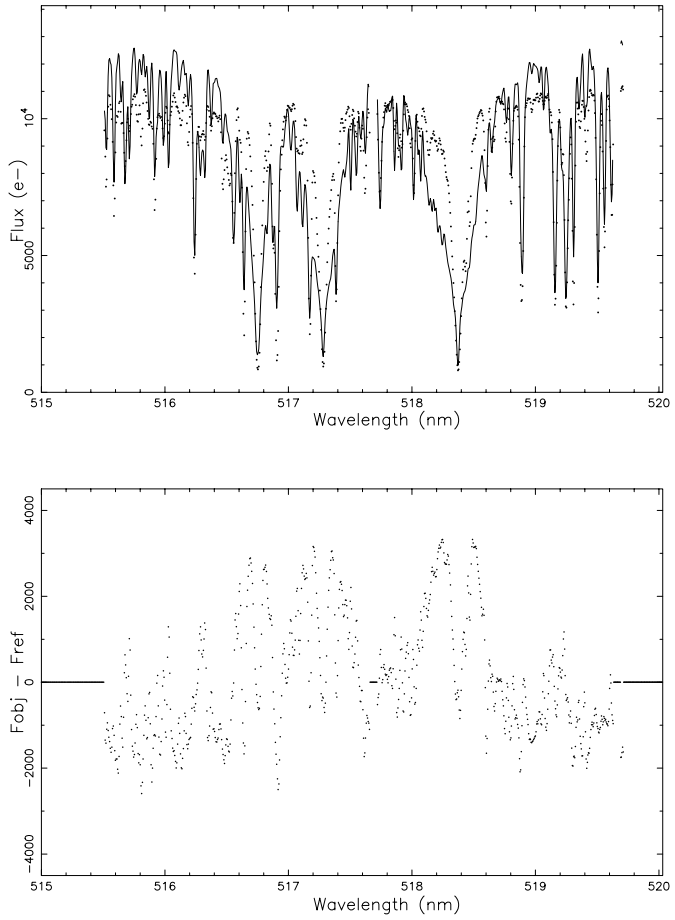

Fig. 5. The upper part of the figure shows the fit between HD 41597, in points, taken as the target ($T_{\rm eff}$ = 4700 K, $\log g$ = 2.38, [Fe/H] = -0.54) and HD 4628 taken as the reference star ($T_{\rm eff}$ = 4960 K, $\log g$ = 4.60, [Fe/H] = -0.29). The lower part shows the difference between their fluxes.

question. First, there is a large variation of the S/N from the blue to the red orders. Second the spectral information contained in each order is unequal.

The first problem is solved by weighting the variance obtained on each order by the the inverse of its mean flux. The degree of ressemblance between the target and the reference star is characterized by the expression :

$$S_k = \frac{1}{N - n_b} \sum_{k \in K} \frac{(n_k - 1) S_k^{'}}{< F_k >}$$

with:

$$N = \sum_{k \in K} n_k$$

where:
K is the set of orders kept in the final result(see the next paragraph), n_b the number of orders contained in K and $< F_k >$ the mean flux of the target star for each order. This expression is in practice equivalent to a reduced χ^2.

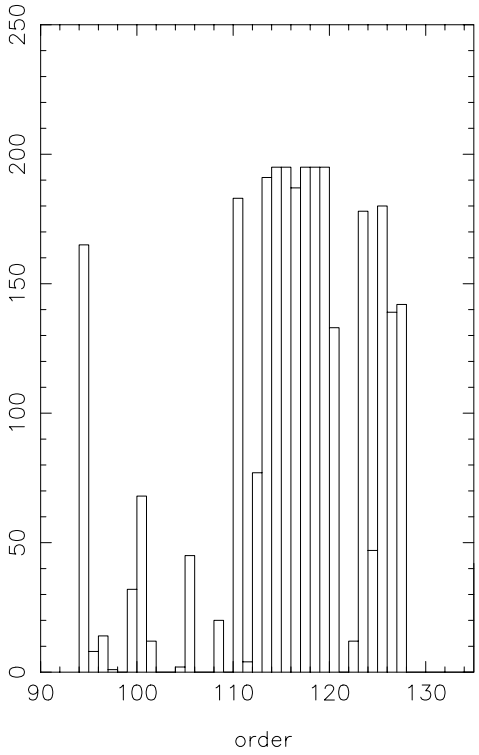

Fig. 6. Relative relevance of each order. The test has been performed by comparing each reference star to the others ($\sim$ 40000 comparisons), by keeping for each comparison the 15 orders which give the highest rms and by counting the occurences of each order in this list.

The second problem is the fact that some orders include strong lines of various elements, whereas some others are almost free of lines. For example, order 119 including the Mg I triplet appears to be one of the most significant orders for every star. Orders 94 and 127 containing H_α and H_β are very useful for effective temperature determinations. Howewer its worth noticing that all orders depend on the three parameters, which can not be estimated independently. The relative relevance of the different orders has been studied. In order to select the best orders for each target. The rms deviation of the fluxes, with respect to the mean flux, caused by spectral lines plus noise, is computed. The 15 orders for which the ratio of this global modulation to pure noise modulation is the highest, are kept. This set of orders changes from one target star to another, but the orders 127, 119 and 94 (including respectively H_β, the Mg I triplet and H_α) are selected in almost every set. The number of 15 has been chosen after a number of "try and see" experiments over various S/N. A larger number of orders introduce noise instead of information. Fig. 6 shows the relative relevance of each order.

For a given target star, the comparison is performed with the 211 reference stars of the library.

The 10 reference stars showing the lowest reduced χ^2 are selected. The solution is given by the weighted mean of the parameters of the reference stars whose reduced χ^2 is lower than 1.11 times the lowest one. The upper limit of 11% has been empirically defined during the phase of test (see Sect. 6)

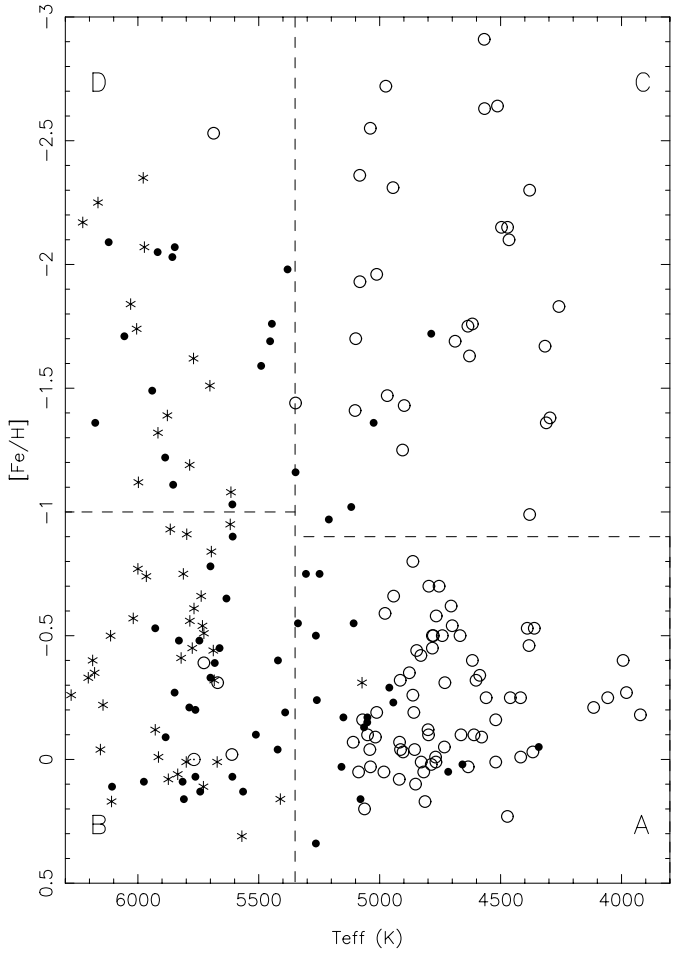

Fig. 7. Distribution of the 211 reference dwarfs, sub-giants and giants in the plane ($T_{\rm eff}$, [Fe/H]). Dots represent dwarfs ($\log g \geq 4.2$), asterisks represent turn-off stars ($4.2 > \log g \geq 3.7$), open circles represent giants ($\log g < 3.7$) and the Sun is represented by its usual symbol. The figure is divided in four zones (from A to D) refered to in Sect. 6.

and is valuable only for target stars with $S/N \geq 30$. For smaller S/N the limit is decreasing (i.e. 1% for S/N = 10).

5. The library of comparison stars

The library is made of 211 well-studied stars in the temperature range [4000 K; 6300 K]. This temperature interval has been chosen because it covers the full span of stars born from the beginning of the Galaxy, with the elimination of stars too cool for having a reliable detailed analysis. The metallicity of these stars is supposed to reflect the metallicity of the interstellar material from which they were formed, tracing the galactic evolution. In hotter stars, the metallicity might be altered by physical processes inside the stars, and spectra of cooler stars are complicated and might lead to erroneous results.

The choice of the reference stars and their atmospheric parameters are fully described in Paper II. A large part of this paper is devoted to homogenizing the parameters because of scattered determinations found in the literature.

The success of our method relies on the existence of a library of high quality, which covers as well as possible the space of the parameters in the considered temperature interval. Fig. 7 shows how dwarfs ($\log g \geq 4.2$), turn-off ($4.2 > \log g \geq 3.7$) and giants stars ($\log g < 3.7$) of the library span the plane ($T_{\rm eff}$,[Fe/H]). As can be seen, the library is not homogeneously filled. The holes in the library reflect the lack of metal deficient stars and cool dwarfs, which are more difficult to observe and to analyse. Of course, in the densest regions of the library the results might be statistically better than in sparse parts. All the spectra of the library have a signal to noise ratio greater than 35, with a mean value of 100. We had to keep in the library a few stars with a low S/N to have enough metal deficient stars, which have fainter magnitudes.

As explained in Sect. 3.5, all the spectra of the library have been convolved to several resolutions. The lowest one correponds to a FWHM of 13.5 km.s^{-1} and is adequate for most of the F5 to K7 stars. For younger stars with higher rotational velocities and broadened lines, TGMET uses versions of the library degraded at lower resolutions.

6. Testing TGMET

The first test was to remove one by one each reference star of the library, treat it like an anonymous object, then compare the estimated parameters and the true ones. This test was performed iteratively to adjust the atmospheric parameters of the reference star as described in Paper II. The overall resulting standard deviation of the estimated versus "true" parameters for this high S/N sample is respectively 86 K, 0.28 dex, 0.16 dex for $T_{\rm eff}$, $\log g$ and [Fe/H].

Several phenomenae influence the results. In metal-rich stars, the amount of spectral information is greater than in almost line free stars. In the same way, stars cooler than 5000 K are losing the Stark profile of the wings of their hydrogen lines. Therefore the uncertainties on the determination of the parameters is greater for the cool and metal-deficient stars than for the hot and metal-rich stars. To take this effect into account, the library was divided in four zones (from A to D, see Fig. 7) and the mean error was calculated as well as the dispersion in each zone and for each parameter. The results are listed in Table 1.

Because our ultimate goal is to use low S/N (~ 10) spectra, the spectra of the library were degraded at S/N = 10 by adding a random (Poisson) noise. The mean error and the dispersion in each zone were recalculated. The results are listed in Table 2.

To be sure that no bias has been introduced with the artificial noise (such as correlation between pixels), the software was tested with 30 stars of well known parameters (some of them already belonging to the library), observed willingly at low S/N. Fig. 8 shows the difference between the true and the estimated parameters as a function of the S/N of the object star.

The computing time for TGMET is about 10 min, when run in parallel with the aquisition and reduction softwares, on the SUN-sparc 20 station devoted to the observations with ELODIE.

Table 1. Statistics on the self-consistency of the library at mean S/N = 100.

Zone	sum	A	B	C	D
number of star	211	87	63	33	28
$< \Delta T_{\rm eff} >$	17	11	9	54	11
$\sigma_{T_{\rm eff}}$	86	74	63	131	87
$< \Delta \log g >$	0.04	0.03	0.03	0.06	0.06
$\sigma_{\log g}$	0.28	0.25	0.20	0.43	0.28
$< \Delta$ [Fe/H]$>$	0.02	0.00	0.00	0.07	0.04
$\sigma_{[Fe/H]}$	0.16	0.14	0.14	0.20	0.19

Table 2. Statistics on the self-consistency of the library at S/N = 10.

Zone	sum	A	B	C	D
number of star	211	87	63	33	28
$< \Delta T_{\rm eff} >$	10	12	-4	50	-9
$\sigma_{T_{\rm eff}}$	102	84	78	158	99
$< \Delta \log g >$	0.03	0.00	0.04	0.08	0.05
$\sigma_{\log g}$	0.29	0.24	0.21	0.45	0.31
$< \Delta$ [Fe/H]$>$	0.02	0.00	0.00	0.07	0.08
$\sigma_{[Fe/H]}$	0.17	0.14	0.14	0.22	0.18

7. Conclusion

The feasibility of a quick determination, at the telescope, of the fundamental atmospheric parameters effective temperature, gravity and metallicity of a star from its spectrum has been demonstrated. This has been done using spectra supplied by the cross-dispersed echelle spectrograph ELODIE, mounted at the coudé focus of the 1.93 m telecope of the Observatoire de Haute-Provence. These spectra have a spectral resolution of 42 000 and cover a large spectral range from 380 to 680 nm. We have been greatly helped by the already installed ELODIE reduction software, supplying on-line the radial velocities and the extracted spectra of the stars.

The method consists in comparing the spectrum of the target star with a library of spectra taken with the same spectrograph, at a typical S/N of 100. Such a library has been assembled, and presently contains the spectra of 211 stars, selected for covering the parameter values encountered in stars belonging to the halo, the thick disk and the old thin disk of the Galaxy. Namely the parameter intervals are [4000K, 6300K], [0.6, 4.7] and [-2.9., 0.35] respectively in $T_{\rm eff}$, $\log g$ and [Fe/H].

A great amount of care has been put into the elimination of all features not intrinsic to the stars before attempting any comparison between their spectra. In particular we have removed the modulation of the spectra by the blaze of the orders (which still exists even if all spectra are taken with the same spectrograph because of the radial velocity shifts), the telluric lines and the hits by cosmic rays. It was also necessary to bring all spectra to a common resolution to avoid differences due to stellar rotation or macroturbulence or to a slight difference in focus during different observing runs. The degree of resemblance between the spectra of the target and those of the library was quantified by a maximum likelihood approach, involving a weighted least-square fit. The parameters of the target star are determined by taking a weighted mean of the the parameters of the most resembling reference stars.

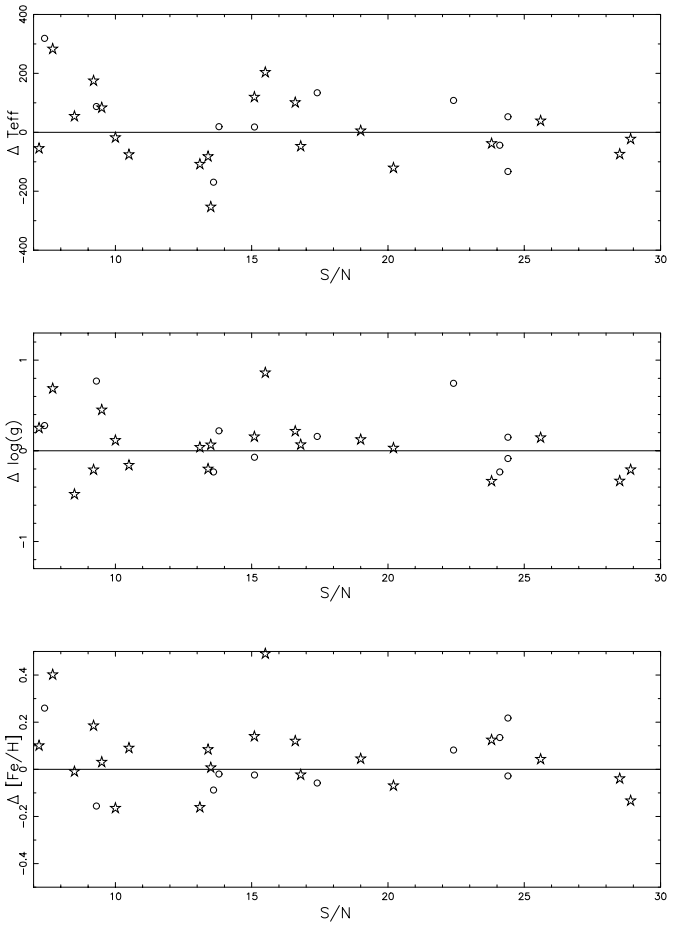

Fig. 8. Difference between true and estimated parameters ($T_{\rm eff}$: upper part, $\log g$: center part, [Fe/H]: lower part) versus S/N for 30 well-known stars used as test stars. Star symbols flag the stars already belonging to the library and which have been reobserved for the purpose of this test at a lower S/N.

The accuracy of the method, with the existing library, has been tested. On the average, the accuracy turns out to be 86 K in $T_{\rm eff}$, 0.28 dex in $\log g$, and 0.16 dex in [Fe/H] for a target spectrum with S/N = 100. This accuracy critically depends upon the number of spectra in the library and the quality of the parameters collected for each reference object in the literature. A second paper (Soubiran et al. 1998) deals with this point in more detail, probing the consistency of the library by internal comparison of all the spectra of the library.

Our fundamental stellar parameter extraction software (named TGMET for Temperature, Gravity, METallicity) is available to all ELODIE users at Observatoire de Haute-Provence. It is online, so that these parameters may be derived during observing runs. Its user-guide is also available on the WEB at http://www.obs-hp.fr.

A similar software is planned for the new spectrograph FEROS at La Silla (ESO).

Future improvements are planned and already under way. The most obvious ones are to fill the sparsely populated zones of the library, and in redetermining the fundamental parameters of the stars which have been spotted as doubtful in the consistency check. Another one is to extend the library of reference stars up to F0, at the request of other observers. In particular the asteroseismologists working on the preselection of target stars for the spatial experiment COROT with ELODIE need atmospheric parameters for stars from A to G type. We plan also to improve the algorithm determining the parameters, by taking more rigorously into account the sensitivity of each pixel of the spectrum to a variation of the parameters. This will be particularly useful for very metal-poor stars, for which only very few places in the spectrum contain useful information. An exciting extension to our software would be to derive abundance ratios in addition to metallicity. For example we could try to determine the alpha-elements to iron ratio, which has been shown to present a scatter larger than believed before (King 1997, Carney et al. 1997, Nissen & Schuster 1997). This ratio is particularly important, as the Mg I green triplet and the molecular band MgH are dominant gravity features. Other abundance ratios of interest as [Ba/Fe], [Sr/Fe] or [Na/Fe] are attractive targets.

Acknowledgements. We are very grateful to Didier Queloz for providing his valuable software for ELODIE's spectra reduction and for fruitful discutions. We want to thank Alain Vin for his constant help during the observational runs. We thank the astronomers who let us use their spectra to fill the library. Many thanks to M.-N. Perrin, C. Sneden and P.E. Nissen for very useful comments and suggestions for improving the manuscript.

References

Baranne, A., Queloz, D., Mayor, M., Adrianzyk, G., Knispel, G., Kohler, D., Lacroix, D., Meunier, J.-P., 1996, A&AS 119, 373
Carney, B.W., Wright, J.S., Sneden, C., Laird, J.B., Aguilar, L.A., Latham, D.W., 1997, AJ 114, 363
Cayrel, R., 1991, in: *Current topics in astrofundamental physics, 1st course*, International School of Astophysics "D. Chalonge", Sanchez N. and Zichichi A. (eds.), p. 655
Cayrel, R., Perrin M.-N., Barbuy B., Buser R., 1991a, A&A 247, 108
Cayrel, R., Perrin M.-N., Buser R., Barbuy B., Coupry M.-F., 1991b, A&A 247, 122
Cuisinier, F., Buser, B., Acker, A., Cayrel, R., Jasniewicz, G., Fresneau, A., 1994, A&A 285, 943
Horne, K. 1986, PASP 98, 609
King, J.R., 1997, AJ 113, 2302
Kurucz, R.L., 1993, CD-ROM 13
Mayor, M., Queloz D., 1995, Nat 378, 355
Moore, C.E., Minnaert, M.G.J., Houtgart, J., 1966, National Bureau of Standards Monograph 61
Nissen, P.E., Schuster, W.J., 1997, A&A 326, 751
Ojha, D.K., Bienaymé, O., Robin, A.C., Mohan, V., 1994, A&A 290, 771
Perrin, M.-N., Friel, E.D., Bienaymé, O., Cayrel, R., Barbuy, B., Boulon, J., 1995, A&A 298, 107
Queloz, D., 1996, ELODIE user's guide, http://www.obs-hp/
Soubiran, C., 1992, A&A 259, 394
Soubiran, C., 1993, A&A 274, 181
Soubiran, C., Katz, D., Cayrel, R., 1998, A&AS in press (Paper II)